Inorg. Chem. **2006**, *45*, 2678–2687

Inorganic Chemistry

Article

Homoleptic Rare Earth Dipyridylamides [$Ln_2(N(NC_5H_4)_2)_6$], Ln = Ce, Nd, Sm, Ho, Er, Tm, Yb, and Sc: Metal Oxidation by the Amine Melt and in 1,2,3,4-Tetrahydroquinoline with the Focus of Different Metal Activation by Amalgams, Liquid Ammonia, and Microwaves

Klaus Müller-Buschbaum* and Catharina C. Quitmann

Institut für Anorganische Chemie, Universität zu Köln, Greinstrasse 6, D-50939 Köln, Germany

Received August 30, 2005

Homoleptic dimeric dipyridylamide complexes of the rare earth elements are obtained by solvent-free oxidation reactions of the metals with melts of 2,2′-dipyridylamine. As the thermal stabilities of the ligand as well as the amide complexes are limiting factors in these high-temperature syntheses, several different metal activation procedures have been investigated: the formation of Ln amalgams and dissolution of the metals in liquid ammonia as well as coupling to microwaves. For comparison with a solvent that shows low solubility of the metals and products, reactions in 1,2,3,4-tetrahydroquinoline were also carried out. For all lanthanides and group 3 metals used homoleptic dimers of the formula [$Ln_2(Dpa)_6$], Ln = Ce (**1**), Nd (**2**), Sm (**3**), Ho (**4**), Er (**5**), Tm (**6**), Yb (**7**), and Sc (**8**) and $Dpa^- = (C_5H_4N)_2N^-$, were obtained, all containing trivalent rare earth ions with a distorted square antiprismatic nitrogen coordination. Due to the large differences in the ionic radii of the metal ions, two different structure types are found that crystallize in the space groups $P2_1/c$ and $P2_1/n$ with the border of the two types being between Tm and Yb. The orientations of two 1,3/1,3-double chelating and linking dipyridylamide ligands ($Dpa^- = (C_5H_4N)_2N^-$) result in different overall orientations of the dimers and thus two structure types. All compounds were identified by single-crystal X-ray analysis. Mid-IR, far IR, and Raman spectroscopy, microanalyses, and simultaneous DTA/TG as well as mass spectrometry regarding their thermal behavior were also carried out to characterize the products. Crystal data for the two types follow. Ce (**1**): $P2_1/n$; $T = 170(2)$ K; $a = 1063.0(1)$, $b = 1536.0(1)$, $c = 1652.0(2)$ pm; $\beta = 101.60(1)°$; $V = 2642.2(3) \times 10^6$ pm^3; R_1 for $F_o > 4\sigma(F_o) = 0.046$, $wR_2 = 0.120$. Sc (**8**): $P2_1/c$; $T = 170(2)$ K; $a = 1073.0(1)$, $b = 1506.2(2)$, $c = 1619.8(2)$ pm; $\beta = 103.16(9)°$; $V = 2548.9(5) \times 10^6$ pm^3; R_1 for $F_o > 4\sigma(F_o) = 0.038$, $wR_2 = 0.091$.

Introduction

As the vast majority of organometallic as well as organoamido chemistry of the lanthanides shows, it is a synthetic challenge to obtain homoleptic nitrogen complexes from classic solvents.[1–4] Certain conditions such as a special ligand design, e.g. by the use of phthalocyanines,[5–7] calix-pyrroles,[8] tripodal amide[9,10] or other multichelating ligands,[11,12] or weakly coordinating anions,[13,14] have to be chosen to avoid

---

* To whom correspondence should be addressed. E-mail: Klaus.Mueller-Buschbaum@uni-koeln.de. Fax: 0049 221 470 5083.

[1] Schumann, H. *Angew. Chem., Int. Ed. Engl.* **1984**, *23*, 474–492; *Angew. Chem.* **1984**, *96*, 475–493.

[2] Schumann, H.; Meese-Marktscheffel, J. A.; Esser, L. *Chem. Rev.* **1995**, *95*, 865–986.

[3] Evans, W. J. *Coord. Chem. Rev.* **2000**, 263–283.

[4] (a) Dehnicke, K.; Greiner, A. *Angew. Chem.* **2003**, *115*, 1378–1392; *Angew. Chem., Int. Ed.* **2003**, *42*, 1340–1354. (b) Kempe, R. *Angew. Chem., Int. Ed.* **2000**, *39*, 468–493; *Angew. Chem.* **2000**, *112*, 478–504.

[5] De Cian, A.; Moussavi, M.; Fischer, J.; Weiss, R. *Inorg. Chem.* **1985**, *24*, 3162–3167.

[6] Haghighi, M. S.; Teske, C. L.; Homborg, H. *Z. Anorg. Allg. Chem.* **1992**, *608*, 73–80.

[7] Darovsky, A.; Wu, L. Y.; Lee, P.; Sheu, H. S. *Acta Crystallogr.* **1991**, *C47*, 1836–1838.

[8] Dube, T.; Gambarotta, S.; Yap, G. P. A. *Angew. Chem.* **1999**, *111*, 1507–1508.

[9] Wietzke, R.; Mazzanti, M.; Latour, J.-M.; Pecaut, J. *J. Chem Soc., Chem. Commun.* **1999**, 209–210.

[10] Natrajan, L.; Pecaut, J.; Mazzanti, M.; LeBrun, C. *Inorg. Chem.* **2005**, *44*, 4756–4765.

[11] Trifonov, A. A.; Bochkarev, M. N.; Schumann, H.; Loebel, J. *Angew. Chem., Int. Ed. Engl.* **1991**, *30*, 1149–1151; *Angew. Chem.* **1991**, *103*, 1170–1172.

[12] Iveson P. B.; Riviere, C.; Guillaneux, D.; Nierlich M.; Thuery, P.; Ephritikhine, M.; Madic, C. *J. Chem. Soc., Chem. Commun.* **2001**, 1512–1513.

10.1021/ic0514795 CCC: $33.50

co-coordination of solvent molecules. In contrast the high-temperature melt synthesis of N-heterocyclic amines with rare earth metals has proved to be a suitable way to obtain homoleptic nonsilyl rare earth amides.[15−24] The solvent-free character of these reactions provides the absence of disturbing coligands. Whereas dipyridylamides of transition metals have been known for some time already,[25−28] complexes of the rare earth elements have only recently been synthesized.[29] For the identical formula [$Ln_2(Dpa)_6$], $Dpa^- = (C_5H_4N)_2N^-$, we reported square antiprismatic nitrogen coordinations for Gd and Yb and a completely different complex 10-fold coordination for La. We can now present the series of trivalent lanthanides as well as the group 3 metal scandium resulting in a variety of three different structure types with the borders being between La and Ce as well as Tm and Yb, respectively. Scandium with the smallest ionic radius also crystallizes in the ytterbium type. The rare earth elements prefer a coordination mode of linking 1,3/1,3-double chelating Dpa ligands, which is different from transition metals that e.g. coordinate via the larger 1,5-chelate or in a chainlike mode (Chart 1). A single 1,3-chelating binding mode like in aminopyridinato complexes[30] is also found for [$Ln_2(Dpa)_6$].[29] As the thermal stability of both the organic amine ligands and the amide products is crucial for this type of reaction, 2,2′-dipyridylamine has been chosen to investigate and focus on different metal activations to drop down the reaction temperatures of high-temperature melt reactions. Here we present the results of amalgam formation[31] and dissolution in liquid ammonia,[32,33] as well as microwave activation of the melt synthesis of rare earth dipyridylamides. To compare this with reactions in solvents that show low solubility concerning the metals and the products, 1,2,3,4-tetrahydroquinoline was used, which does not form rare earth complexes itself.

Chart 1. Coordination Modes of 2,2-Dipyridylamido Groups (DpaH = $(C_5H_4N)_2NH$, Dpa^- = Dipyridylamide $(C_5H_4N)_2N^-$) and Aminopyridinato Ligands (C): 1,3/1,3-Double Chelate (A); Nonchelating (B); 1, 3-Chelate (C); 1,5-Chelate (D)

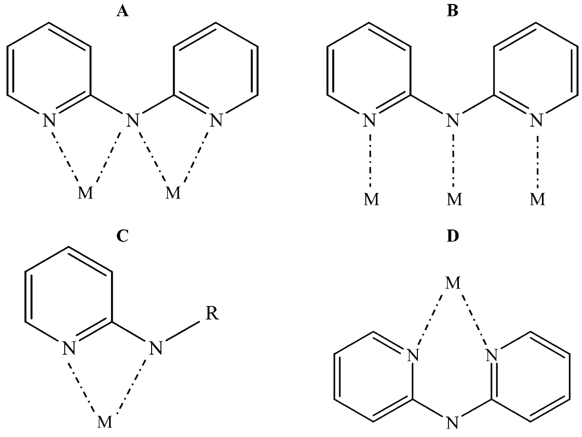

Experimental Section

General Data. All manipulations were carried out under inert atmospheric conditions using glovebox and ampule as well as vacuum line techniques. Heating furnaces with Al_2O_3 tubes together with Eurotherm 2416 control elements were used for the ampule experiments. The IR spectra were recorded using a Bruker FTIR-IS66V-S spectrometer, and the Raman spectra were recorded using a Bruker FRA 106-S spectrometer. For mid-IR investigations KBr pellets were used, and PE pellets for far-IR were used under vacuum. The thermal decompositions of **4**−**7** and [$La_2(N(NC_5H_4)_2)_6$]-(**9**)[29] were studied using simultaneous DTA/TG (Netzsch STA-409). Thereby both the bulk products of the melt reactions as well as products purified by either washing excess ligand off with toluene or evaporating excess DpaH (at 230 °C) were investigated. A 30.0 mg amount of the bulk product of the Ho reaction (**4**), 21.2 mg for Tm (**6**), 22.0 mg for Yb (**7**), and 20.9 mg for La (**9**), was heated from 20 up to 700 °C at a heating rate of 10 °C/min in a constant Ar flow of 60 mL/min. A 14.7 mg amount of the purified Ho-containing product (**4**) and 18.5 mg of the purified Tm-containing product (**6**) were also treated by heating from 20 up to 700 °C at a heating rate of 10 °C/min in a constant Ar flow of 60 mL/min simultaneously investigated by DTA/TG. The thermal properties of the Er-containing compound **5** were further investigated on 49.3 mg by mass spectrometry (Balzers QMS 421 quadropole mass spectrometer, 0.2 s scanning time/mass) simultaneously with DTA/TG.

For the microwave activation a usual pulsed microwave generator of 1200 W with a copper tube inlet and a quartz tube were used. The hot spots of the microwave were defined by the use of coupling to carbon powder prior to investigation of the oxidation reaction. The ampule containing the reaction mixture was placed inside the quartz tubes and within the range of one of the hot spots. Hg (Riedel-de-Haen) of 99.99% purity was used for amalgam activation, and ammonia (Linde, 99.9999%), for dissolution activation. 1,2,3,4-Tetrahydroquinoline (Acros, 98%), 2,2′-dipyridylamine (Aldrich, 98%), and the rare earth metals (Chempur, >99%) were used as purchased.

Reactions of all metals used without any activation under otherwise identical conditions could not be observed prior to decomposition except for Yb, which made an increase of 45 °C reaction temperature necessary compared to the use of Hg.

---

(13) Piguet, C.; Williams, A. F.; Bernardinelli, G.; Bünzli, J.-C. G. *Inorg. Chem.* **1993**, *32*, 4139−4149.

(14) Petoud, S.; Bünzli, J.-C. G.; Renaud, F.; Piguet, C.; Schenk, K. J.; Hopfgartner, G. *Inorg. Chem.* **1997**, *36*, 5750−5760.

(15) Deacon, G. B.; Gitlits, A.; Skelton, B. W.; White, A. H. *J. Chem Soc., Chem. Commun.* **1999**, 1213−1214.

(16) Deacon, G. B.; Gitlits, A.; Roesky, P. W.; Bürgstein, M. R.; Lim, K. C.; Skelton, B. W.; White, A. H. *Chem.*—Eur. J. **2001**, *7*, 127−138.

(17) Müller-Buschbaum, K. *Z. Anorg. Allg. Chem*. **2002**, *628*, 2731−2737.

(18) Müller-Buschbaum, K.; Quitmann, C. C. *Inorg. Chem*. **2003**, *42*, 2742−2750.

(19) Müller-Buschbaum, K.; Quitmann, C. C. *Z. Anorg. Allg. Chem*. **2004**, *630*, 131−136.

(20) Müller-Buschbaum, K.; Quitmann, C. C. *Eur. J. Inorg. Chem*. **2004**, 4330−4337.

(21) Quitmann, C. C.; Müller-Buschbaum, K. *Z. Naturforsch*. **2004**, *59b*, 562−566.

(22) Deacon, G. B.; Forsyth, C. M.; Gitlits, A.; Skelton, B. W.; White, A. H. *J. Chem. Soc. Dalton Trans.* **2004**, 1239−1247.

(23) Müller-Buschbaum, K. *Z. Anorg. Allg. Chem*. **2005**, *631*, 811−828.

(24) Freeman, H. C.; Snow, M. R. *Acta Crystallogr.* **1965**, *18*, 843−845.

(25) Johnson, J. E.; Jacobson, R. A. *J. Chem Soc., Dalton Trans.* **1973**, 580−584.

(26) Ray, N.; Hathaway, B. *J. Chem. Soc., Dalton Trans.* **1980**, 1105−1111.

(27) Youngme, S.; Poopasit, K.; Chinnakali, K.; Chantrapromma, S.; Fun, H.-K. *Inorg. Chim. Acta* **1999**, *292*, 57−63.

(28) Cotton, F. A.; Daniels, L. M.; Murillo, C. A.; Zhou, H.-C. *Inorg. Chim. Acta* **2000**, *305*, 69−74.

(29) Müller-Buschbaum, K. *Z. Anorg. Allg. Chem*. **2003**, *629*, 2127−2132.

(30) Spangenberg, A.; Arndt, P.; Kempe, R. *Angew. Chem., Int. Ed.* **1998**, *37*, 832; *Angew. Chem.* **1998**, *110*, 824.

(31) Magyar, B. *Inorg. Chem.* **1968**, *7*, 1457−1462.

(32) Juza, R.; Hadenfeldt, C. *Naturwissenschaften* **1968**, *55*, 229.

(33) Hadenfeldt, C.; Juza, R. *Naturwissenschaften* **1969**, *56*, 282.

Yield determinations result from weighing of either (a) evaporating excess DpaH for amalgam and ammonia activation or (b) washing off the Tech and thus excess DpaH with hexane or toluene in cases in which 1,2,3,4-tetrahydroquinoline and microwave activations were used. All products are higly air and moisture sensitive.

$[Ce_2(N(NC_5H_4)_2)_6]$ (1). Amalgam Activation. Ce (0.5 mmol = 70 mg) and 2,2′-dipyridylamine (DpaH, 1.5 mmol = 262 mg) together with Hg (0.2 mmol = 40 mg) were sealed in an evacuated Duran glass ampule and heated to 150 °C for 4 h and to 175 °C for another 2.5 h. This temperature was held for 168 h. The reaction mixture was then cooled to 70 °C over 300 h and to room temperature within 20 h. Except for a slight amount of the reactants and the activating Hg, the reaction was complete resulting in highly reflecting yellow crystals of the product. Yield: 290 mg = 90%.

Tetrahydroquinoline Solution. Ce (0.5 mmol = 70 mg) and 2,2′-dipyridylamine (DpaH, 1.5 mmol = 262 mg) together with tetrahydroquinoline (1.5 mmol = 200 mg) were degassed and sealed in an evacuated Duran glass ampule and heated to 140 °C for 6 h and to 170 °C for another 1.5 h. This temperature was held for 168 h. The reaction mixture was then cooled to 90 °C over 180 h and to room temperature within 12 h. Except for a slight amount of the reactants and the tetrahydroquinoline, the reaction was complete resulting in reflecting gray to violet crystals of the product. Yield: 278 mg = 86%. Anal. Calcd for $C_{60}H_{48}N_{18}Ce_2$ (M_r = 1301.39 g mol^{-1}): C, 55.38; N, 19.37; H, 3.72. Found: C, 55.2; N, 18.8; H, 3.8. MIR (KBr): 3015 m, 2932 m, 1605 s, 1567 s, 1528 s, 1481 s, 1463 m, 1436 vs, 1342 m, 1332 m, 1313 s, 1275 w, 1148 s, 1103 w, 1050 w, 990 m, 908 w, 874 w, 769 vs, 735 m cm^{-1}. Far-IR (PE): 594 w, 552 m, 542 m, 525 w, 498 w, 407 w, 353 w, 286 w, 273 vw, 235 w, 222 w, 207 m, 194 m, 180 m, 166 s, 155 m, 141 w, 88 w, 74 m cm^{-1}. Raman: 1600 vs, 1550 s, 1422 m, 1370w, 1308 w, 1256 s, 1250 ssh, 1151,w, 1106 w, 1044s, 995 vs, 982 vs, 769 w, 862 m, 617 w, 111 s, 82 s cm^{-1}.

$[Nd_2(N(NC_5H_4)_2)_6]$ (2). Amalgam Activation. Nd (0.5 mmol = 72 mg) and 2,2′-dipyridylamine (1.5 mmol = 262 mg) together with Hg (0.2 mmol = 40 mg) were sealed in an evacuated Duran glass ampule and heated to 170 °C for 8 h and to 190 °C for another 5 h. This temperature was held for 168 h. The reaction mixture was then cooled to 90 °C over 300 h and to room temperature within 6 h. Except for a slight amount of the reactants and the activation mercury, the reaction was complete resulting in reflecting violet crystals of the product. Yield: 272 mg = 83%.

Tetrahydroquinoline Solution. Nd (0.5 mmol = 72 mg) and 2,2′-dipyridylamine (DpaH, 1.5 mmol = 262 mg) together with tetrahydroquinoline (1.5 mmol = 200 mg) were degassed and sealed in an evacuated Duran glass ampule and heated to 150 °C for 5 h and to 175 °C for another 1.5 h. This temperature was held for 168 h. The reaction mixture was then cooled to 90 °C over 85 h and to room temperature within 14 h. Except for a slight amount of the reactants and the tetrahydroquinoline, the reaction was complete resulting in reflecting gray to violet crystals of the product. Yield: 268 mg = 82%. Anal. Calcd for $C_{60}H_{48}N_{18}Nd_2$ (M_r = 1305.63 g mol^{-1}): C, 55.03; N, 19.25; H, 3.70. Found: C, 54.9; N, 19.0; H, 3.6. MIR (KBr): 30015 m, 2926 m, 1596 s, 1580 s, 1550 s, 1460 vs, 1429 vs, 1370 s, 1330 s, 1309 m, 1298 s, 1285 s, 1243 m, 1174 vs, 1108 m, 1041 m, 996 s, 983 m, 831 s, 769 vs, 733 s cm^{-1}. Far-IR (PE): 594 w, 528 m, 514 w, 498 w, 409 w, 403 w, 359 w, 289 w, 244 w, 232 w, 208 vw, 194 vw, 174 m, 169 msh, 100 w cm^{-1}.

$[Sm_2(N(NC_5H_4)_2)_6]$ (3). Amalgam Activation. Sm (0.2 mmol = 38 mg) and 2,2′-dipyridylamine (1 mmol = 171 mg) together with Hg (0.2 mmol = 40 mg) were sealed in an evacuated Duran glass ampule and heated to 180 °C for 5.5 h and to 220 °C for another 2.5 h. This temperature was held for 168 h. The reaction mixture was then cooled to 90 °C over 300 h and to room temperature within 6 h. Except for a slight amount of the reactants and the activation mercury, the reaction was complete resulting in reflecting yellow crystals of the product. Yield: 121 mg = 91%.

Tetrahydroquinoline Solution. Sm (0.5 mmol = 72 mg) and 2,2′-dipyridylamine (1.5 mmol = 262 mg) together with tetrahydroquinoline (2 mmol = 260 mg) were degassed and sealed in an evacuated Duran glass ampule and heated to 180 °C for 6 h and to 210 °C for another 3 h. This temperature was held for 168 h. The reaction mixture was then cooled to 60 °C over 480 h and to room temperature within 6 h. Except for a slight amount of the reactants and the tetrahydroquinoline, the reaction was complete resulting in reflecting yellow crystal plates of the product. Yield: 278 mg = 84%. Anal. Calcd for $C_{60}H_{48}N_{18}Sm_2$ (M_r = 1321.88 g mol^{-1}): C, 54.52; N, 19.07; H, 3.66. Found: C, 54.7; N, 19.0; H, 3.5. MIR (KBr): 2990 w, 1596 s, 1581 s, 1551 m, 1525 m, 1462 vs, 1430 vs, 1370 m, 1334 m, 1310 m, 1298 m, 1285 m, 1243 m, 1148 s, 998 s, 982 m, 770 vs, 735 m cm^{-1}. Far-IR (PE): 594 m, 544 m, 536 m, 524 s, 498 m, 427 w, 410 s, 403 m, 347 w, 290 w, 275 w, 249 m, 205 vs, 195 vs, 178 s, 157 m, 84 w, 71 w cm^{-1}. Raman: 1600 m, 1422 w, 1240 w, 1151,w, 1106 w, 1044 m, 998 s, 983 vs, 908 w, 828 w, 771 w, 678 m, 628 w, 193 w, 108 msh, 82 s cm^{-1}.

$[Ho_2(N(NC_5H_4)_2)_6]$ (4). Microwave Activation. Ho (1 mmol = 165 mg) and 2,2′-dipyridylamine (3 mmol = 513 mg) were sealed in an evacuated Duran glass ampule and brought into the hot spot of a 1200 W microwave. The microwave radiation was put on for three subsequent intervals of 5 s each resulting in immediate heating of the metal visible by an intense red light. The metal was surrounded by a gray-yellow solid. Longer microwave intervals resulted in decomposition of the ligand. The reaction mixture was then heated to 190 °C for 6 h and to 210 °C for another 2 h. This temperature was held for 168 h. The reaction mixture was then cooled to 90 °C over 400 h and to room temperature within 6 h. Except for a slight amount of the reactants the reaction was complete resulting in a brown to yellow solid of yellow-grey crystals of the product. Yield: 542 mg = 80%.

Amalgam Activation. Ho (1 mmol = 165 mg) and 2,2′-dipyridylamine (3 mmol = 513 mg) together with Hg (0.2 mmol = 40 mg) were sealed in an evacuated Duran glass ampule and heated to 180 °C for 5.5 h and to 210 °C for another 2.5 h. This temperature was held for 168 h. The reaction mixture was then cooled to 90 °C over 400 h and to room temperature within 8 h. Except for a slight amount of the reactants and the activation mercury, the reaction was complete resulting in reflecting yellow-grey crystals of the product. Yield: 529 mg = 78%. Anal. Calcd for $C_{60}H_{48}N_{18}Ho_2$ (M_r = 1355.02 g mol^{-1}): C, 53.34; N, 18.66; H, 3.58. Found: C, 53.1; N, 18.9; H, 3.9. MIR (KBr): 3017 m, 1599 vs, 1582 vs, 1552 s, 1531 m, 1463 vs, 1422 vs, 1368 m, 1350 m, 1336 s, 1312 m, 1299 m, 1285 m, 1245 m, 1148 s, 999 s, 980 m, 769 vs, 733 m cm^{-1}. Far-IR (PE): 595 w, 546 m, 540 m, 532 w, 498 vw, 412 m, 405 msh, 351 vw, 278 vw, 254 w, 236 vw, 205 m, 195 m, 175 m, 154 w, 72 w cm^{-1}. Raman: 3055 vs, 1601 s, 1419 w, 1276 s, 1252 m, 1151 w, 1105 w, 1052 m, 988 vs, 983 vs, 205 m, 111 vs, 90 ssh cm^{-1}. DTA/TG, bulk product (Ar): 85 °C, mp DpaH (expt 90 °C) 235°C, bp DpaH (expt 238 °C), measured 22% mass loss; 335 °C, mp $[Ho_2(N(NC_5H_4)_2)_6]$; 410 °C, decomposition $[Ho_2(N(NC_5H_4)_2)_6]$, measured 10% mass loss. DTA/TG, crystalline **4** (Ar): 235 °C, bp DpaH (expt 238 °C), measured 6% mass loss; 335 °C, mp $[Ho_2(N(NC_5H_4)_2)_6]$; 410 °C, decomposition $[Ho_2(N(NC_5H_4)_2)_6]$, measured 22% mass loss.

[$Er_2(N(NC_5H_4)_2)_6$] (5). Microwave Activation. Er (0.5 mmol = 84 mg) and 2,2′-dipyridylamine (1.5 mmol = 262 mg) were sealed in an evacuated Duran glass ampule and brought into the hot spot of a 1200 W microwave. The microwave radiation was put on for four subsequent intervals of 5 s each resulting in immediate heating of the metal visible by an intense red light. The metal was surrounded by a gray-brown solid. Longer microwave intervals resulted in decomposition of the ligand. The reaction mixture was then heated to 180 °C for 6 h and to 190 °C for another 4 h. This temperature was held for 168 h. The reaction mixture was then cooled to 90 °C over 400 h and to room temperature within 6 h. Except for a slight amount of the reactants, the reaction resulted in a gray-brown to yellow solid of decomposed ligand and gray crystals of the product. Yield: 141 mg = 42%.

Amalgam Activation. Er (1 mmol = 167 mg) and 2,2′-dipyridylamine (3 mmol = 513 mg) together with Hg (0.15 mmol = 30 mg) were sealed in an evacuated Duran glass ampule and heated to 130 °C for 7 h and to 175 °C for another 22 h. This temperature was held for 96 h. The reaction mixture was then cooled to 80 °C over 190 h and to room temperature within 12 h. Except for a slight amount of the reactants and the activation mercury, the reaction was complete resulting in reflecting almost colorless crystals of the product. Yield: 557 mg = 82%. Anal. Calcd for $C_{60}H_{48}N_{18}Er_2$ (M_r = 1359.68 g mol^{-1}): C, 52.99; N, 18.53; H, 3.53. Found: C, 52.3; N, 18.3; H, 3.6. MIR (KBr): 3128 s, 1597 s, 1582 s, 1553 m, 1524 m, 1463 s, 1438 vs, 1430 vs, 1422 vssh, 1401 vs, 1338 m, 1313 m, 1300 m, 1285 w, 1245 w, 1148 m, 999 m, 770 s, 730 m cm^{-1}. Far-IR (PE): 594 w, 540 m, 531 m, 512 w, 498 w, 412 m, 401 msh, 350 w, 255 m, 247 w, 205 m, 192 m, 174 w, 155 m, 83 w, 71 w cm^{-1}. DTA/TG, bulk product (Ar): 80 °C, mp DpaH (expt 90 °C); 240 °C, bp DpaH (expt 238 °C), measured 19% mass loss; 320 °C, mp [$Er_2(N(NC_5H_4)_2)_6$]; 385 °C, decomposition [$Er_2(N(NC_5H_4)_2)_6$], measured 12% mass loss. MS (*m*/*z*): $C_5H_5N)_2NH^+$, 171; $C_5H_5N^+$, 79; $C_5H_4N^+$, 78; $C_4H_4N^+$, 67; $C_4H_4{}^+$, 52; $C_4H_3{}^+$, 51; $C_2H_3N^+$/$NCHN^+$, 41; $C_3H_3{}^+$, 39; $C_3H_2{}^+$, 38; $C_2H_3{}^+$/HCN^+, 27; $NH_3{}^+$, 17; $NH_2{}^+$, 16; NH^+, 15.

[$Tm_2(N(NC_5H_4)_2)_6$] (6). Amalgam Activation. Tm (0.5 mmol = 85 mg) and 2,2′-dipyridylamine (1.2 mmol = 212 mg) together with Hg (0.15 mmol = 30 mg) were sealed in an evacuated Duran glass ampule and heated to 130 °C for 7 h and to 175 °C for another 22 h. This temperature was held for 96 h. The reaction mixture was then cooled to 80 °C over 190 h and to room temperature within 12 h. Except for a slight amount of the reactants and the activation mercury, the reaction was complete resulting in reflecting almost colorless crystals of the product. Yield: 257 mg = 94%.

Tetrahydroquinoline Solution. Tm (0.5 mmol = 85 mg) and 2,2′-dipyridylamine (1.5 mmol = 262 mg) together with tetrahydroquinoline (2 mmol = 260 mg) were degassed and sealed in an evacuated Duran glass ampule and heated to 160 °C for 6 h and to 170 °C for another 3 h. This temperature was held for 168 h. The reaction mixture was then cooled to 80 °C over 168 h and to room temperature within 6 h. Except for a slight amount of the reactants and the tetrahydroquinoline, the reaction was complete resulting in reflecting colorless crystals of the product. Yield: 254 mg = 93%. Anal. Calcd for $C_{60}H_{48}N_{18}Tm_2$ (M_r = 1363.02 g mol^{-1}): C, 52.87; N, 18.49; H, 3.52. Found: C, 52.3; N, 18.2; H, 3.4. MIR (KBr): 3013 w, 1600 s, 1581 s, 1554 m, 1463 vs, 1419 vs, 1423 vs, 1377 m, 1368 m, 1340 m, 1312 m, 1299 m, 1147 m, 1000 m, 984 w, 770 s, 734 m cm^{-1}. Far-IR (PE): 596 vw, 541 m, 532 m, 513 vw, 500 vw, 412 m, 352 w, 267 w, 257 w, 205 m, 196 m, 165 w, 146 w, 106 w, 73 w cm^{-1}. Raman: 3063 m, 1604 s, 1555 m, 1426 m, 1375w, 1259 m, 1044 s, 1001 m, 983 s, 686 w, 106 m, 82 s cm^{-1}. DTA/TG, bulk product (Ar): 80 °C, mp DpaH (expt 90°C); 225 °C, bp DpaH (expt 238 °C), measured 6% mass loss; 320 °C, mp [$Tm_2(N(NC_5H_4)_2)_6$]; 395 °C, decomposition [$Tm_2(N(NC_5H_4)_2)_6$], measured 21% mass loss. DTA/TG, crystalline **6** (Ar): 230 °C, bp DpaH (expt 238 °C), measured 3% mass loss; 315 °C, mp [$Tm_2(N(NC_5H_4)_2)_6$]; 390 °C, decomposition [$Tm_2(N(NC_5H_4)_2)_6$], measured 24% mass loss.

[$Yb_2(N(NC_5H_4)_2)_6$] (7). Microwave Activation. Yb (1 mmol = 173 mg) and 2,2′-dipyridylamine (3 mmol = 513 mg) were sealed in an evacuated Duran glass ampule and brought into the hot spot of a 1200 W microwave. The microwave radiation was put on for three subsequent intervals of 5 s each resulting in immediate heating of the metal visible by an intense red light. The metal was surrounded by a brown-yellow solid. Longer intervals resulted in decomposition of the ligand. The reaction mixture was then heated to 170 °C for 6 h and to 190 °C for another 30 h. This temperature was held for 168 h. The reaction mixture was then cooled to 90 °C over 300 h and to room temperature within 6 h. Except for a slight amount of the reactants, the reaction was complete resulting in a yellow solid of yellow crystals of the product. Yield: 602 mg = 88%.

Ammonia Activation. Yb (1 mmol = 173 mg) was filled an ampule and 6 mL of ammonia condensed in by the use of liquid nitrogen. Slow increase of temperature >−78 °C gave a blue colored solution of the metal in liquid ammonia. Further heating to room temperature in 4 h resulted in a bronze metal mirror on the glass walls first, which turned into very fine particles of Yb upon complete ammonia evaporation. 2,2′-Dipyridylamine (3 mmol = 513 mg) was then filled into this ampule, and it was sealed under vacuum and heated to 180 °C for 5.5 h and to 210 °C for another 1.5 h. This temperature was held for 124 h. The reaction mixture was then cooled to 90 °C over 100 h and to room temperature within 8 h. The reaction was almost complete resulting in a completely crystalline yellow bulk of the product. Yield: 581 mg = 85%. Anal. Calcd for $C_{60}H_{48}N_{18}Yb_2$ (M_r = 1367.24 g mol^{-1}): C, 52.73; N, 18.44; H, 3.51. Found: C, 52.6; N, 18.2; H, 3.5. MIR (KBr): 3014 m, 3003 m, 2926 m, 1600 s, 1580 s, 1555 m, 1529 m, 1463 vs, 1438 vs, 1433 vssh, 1427 vssh, 1378 m, 1368 m, 1341 s, 1313 m, 1299 m, 1283 m, 1258 m, 1246 m, 1146 s, 1109 w, 1042 w, 1014 msh, 1001 s, 985 s, 951 w, 912 m, 860 w, 835 m, 769 vs, 733 s, 623 w cm^{-1}. Far-IR (PE): 570 w, 548 m, 540 wsh, 514 w, 482 w, 433 w, 415 w, 359 m, 289 w, 205 vw, 191 m, 182 m, 158 w, 69 w cm^{-1}.

Amalgam Activation. The synthesis was carried out according to the literature.[29] The reaction without activation under otherwise identical conditions could not be observed prior to decomposition. Yield: 71%.

[$Sc_2(N(NC_5H_4)_2)_6$] (8). Tetrahydroquinoline Solution. Sc (1 mmol = 45 mg) and 2,2′-dipyridylamine (3 mmol = 513 mg) together with tetrahydroquinoline (2 mmol = 260 mg) were degassed and sealed in an evacuated Duran glass ampule and heated to 150 °C for 5.5 h and to 180 °C for another 3 h. This temperature was held for 168 h. The reaction mixture was then cooled to 90 °C over 180 h and to room temperature within 24 h. Except for a slight amount of the reactants and the tetrahydroquinoline, the reaction was complete resulting in reflecting light yellow crystal needles of the product. Yield: 444 mg = 80%.

Amalgam Activation. Sc (1 mmol = 45 mg) and 2,2′-dipyridylamine (2 mmol = 342 mg) together with Hg (0.15 mmol = 30 mg) were sealed in an evacuated Duran glass ampule and heated to 170 °C for 5 h and to 190 °C for another 2 h. This temperature was held for 168 h. The reaction mixture was then cooled to 90 °C over 330 h and to room temperature within 12 h. Except for a slight amount of the reactants and the activation

Table 1. Crystallographic Data for $[Ln_2(Dpa)_6]$, Ln = Ce (**1**), Nd (**2**), Sm (**3**), Ho (**4**), Er (**5**), Tm (**6**), Yb (**7**), and Sc (**8**) and $Dpa^- = (C_5H_4N)_2N^-$ (Deviations in Parentheses)

param	**1**	**2**	**3**	**4**	**5**	**6**	**7**	**8**
formula	$C_{60}H_{48}N_{18}Ce_2$	$C_{60}H_{48}N_{18}Nd_2$	$C_{60}H_{48}N_{18}Sm_2$	$C_{60}H_{48}N_{18}Ho_2$	$C_{60}H_{48}N_{18}Er_2$	$C_{60}H_{48}N_{18}Tm_2$	$C_{60}H_{48}N_{18}Yb_2$	$C_{60}H_{48}N_{18}Sc_2$
fw	1301.39	1305.63	1321.88	1355.02	1359.68	1363.02	1367.24	1111.08
cryst system	monoclinic	monoclinic	monoclinic	monoclinic	monoclinic	monoclinic	monoclinic	monoclinic
space group	$P2_1/n$	$P2_1/n$	$P2_1/n$	$P2_1/n$	$P2_1/n$	$P2_1/n$	$P2_1/c$	$P2_1/c$
a/pm	1063.0(1)	1067.7(2)	1073.3(2)	1073.5(2)	1074.3(3)	1073.85(8)	1070.7(2)	1073.0(1)
b/pm	1536.0(1)	1532.9(2)	1527.4(2)	1517.5(3)	1513.3(5)	1514.2(2)	1529.9(2)	1506.2(2)
c/pm	1652.0(2)	1644.4(3)	1635.7(2)	1621.3(3)	1618.2(4)	1617.8(2)	1645.1(2)	1619.8(2)
β/deg	101.60(1)	101.30(1)	100.23(1)	100.85(3)	100.82(2)	100.74(1)	103.80(1)	103.16(9)
$V/10^6$ pm^3	2642.2(3)	2639.0(6)	2622.8(5)	2594.1(9)	2583.8(9)	2584.6(4)	2616.8(5)	2548.9(5)
Z	2	2	2	2	2	2	2	2
d_{calc}/g cm^{-1}	1.636	1.648	1.674	1.730	1.743	1.746	1.735	1.448
μ/cm^{-1}	17.6	20.1	22.8	30.9	32.9	34.7	36.1	3.3
T/K	170(2)	170(2)	170(2)	170(2)	170(2)	170(2)	170(2)	170(2)
data range	$3.66 \le 2\theta \le 59.24$	$3.66 \le 2\theta \le 54.54$	$3.68 \le 2\theta \le 54.56$	$3.70 \le 2\theta \le 63.46$	$3.72 \le 2\theta \le 50.00$	$3.72 \le 2\theta \le 54.60$	$3.68 \le 2\theta \le 54.68$	$3.74 \le 2\theta \le 54.60$
X-ray radiatn	Mo Kα, λ = 71.073	Mo Kα, λ = 71.073	Mo Kα, λ = 71.073	Mo Kα, λ = 71.073	Mo Kα, λ = 71.073	Mo Kα, λ = 71.073	Mo Kα, λ = 71.073	Mo Kα, λ = 71.073
no. of unique reflcns	7380	5786	5804	5753	4496	5728	5845	5656
no. of params	457						457	
R_1[a] for n reflcns $F_o > 4\sigma(F_o)$; n	0.046; 5194	0.036; 4395	0.035; 4409	0.039; 4337	0.069; 2618	0.030; 4536	0.038; 4524	0.038; 3761
R_1 (all)	0.065	0.056	0.054	0.059	0.131	0.041	0.054	0.069
wR_2[b] (all)	0.120	0.092	0.090	0.101	0.161	0.074	0.108	0.091
electron density /e10^6 pm^{-1}	+1.4/−1.9	+1.1/−1.3	+0.8/−1.6	+1.0/−1.1	+0.3/−1.1	+0.7/−1.4	+1.3/−1.2	+0.3/−0.5

[a] $R_1 = \sum[|F_o| - |F_c|]/\sum[|F_o|$. [b] $wR_2 = (\sum w(F_o^2 - F_c^2)^2/(\sum w(F_o^4))^{1/2}$.[32]

mercury, the reaction was complete resulting in reflecting light yellow crystals of the product. Yield: 281 mg = 76%. Anal. Calcd for $C_{60}H_{48}N_{18}Sc_2$ (M_r = 1111.08 g mol^{-1}): C, 64.86; N, 22.68; H, 4.32. Found: C, 64.6; N, 22.3; H, 4.6. MIR (KBr): 3030 w, 1602 s, 1581 s, 1556 m, 1478 s, 1464 vs, 1422 vs, 1377 m, 1365 m, 1352 m, 1313 m, 1298 m, 1284 m, 1147 m, 1000 m, 984 m, 773 s, 736 m cm^{-1}. Far-IR (PE): 598 vw, 549 w, 542 m, 532 w, 415 msh, 410 m, 387 w, 366 m, 329 m, 309 m, 264 w, 244 msh, 234 m, 216 m, 185 w cm^{-1}.

$[La_2(N(NC_5H_4)_2)_6]$ (9). Amalgam Activation. $[La_2(N(NC_5H_4)_2)_6]$ was prepared according to the literature.[29] Yield: 84%. DTA/TG, bulk product (Ar): 85 °C, mp DpaH (expt 90 °C); 230 °C, bp DpaH (expt 238 °C), measured 16% mass loss; 280 °C, mp $[La_2(N(NC_5H_4)_2)_6]$; 340 °C, decomposition $[La_2(N(NC_5H_4)_2)_6]$, measured 14% mass loss.

X-ray Crystallographic Studies. The best out of three single crystals of each of the compounds $[Ln_2(Dpa)_6]$, Ln = Ce (**1**), Ho (**4**), and Tm (**6**), and the best of out five crystals for Ln = Nd (**2**), Sm (**3**), Er (**5**), Yb (**7**), and Sc (**8**) were selected for single-crystal X-ray investigations under glovebox conditions and sealed in glass capillaries. All data collections were carried out on a STOE IPDS-II diffractometer at 170 K (Mo Kα radiation, λ = 0.7107 Å). For all eight compounds the structure was determined using direct methods.[34] All non-H atoms were refined anisotropically by least-squares techniques.[35] The hydrogen positions were completely retrieved from the differential Fourier card and refined isotropically. The compounds $[Ln_2(Dpa)_6]$ with Ln = Ce (**1**)−Tm (**6**) crystallize in the monoclinic space group $P\,2_1/n$ (type II), and the compounds $[Ln_2(Dpa)_6]$ with Ln = Yb (**7**) and Sc (**8**), in the monoclinic space group $P2_1/c$ (according to type III). Transformation of type II into a comparable setting according to type II ($P2_1/c$) is only possible by an additional translation of 0.5 along the c-axis and results in large β angles close to and beyond 120° but does not lead to identical structures. A cell transformation preserves the two structure types; viz., atom positions of one type cannot be transferred to the other and refined successfully. For comparable views of the crystal structures of the two types, the nonstandard setting $P2_1/n$ for type II is kept for Yb (**7**) and Sc (**8**). Crystallographic data are summarized in Table 1. Further information was deposited at the Cambridge Crystallographic Data Centre, CCDC, 12 Union Road, Cambridge CB2 1EZ, U.K. (fax +44 1223336033 or e-mail deposit@ccdc.cam.ac.uk) and may be requested by citing the deposition numbers CCDC-248665 (**1**), -282287 (**2**), -248666 (**3**), -282289 (**4**), -282288 (**5**), -282291 (**6**), -282292 (**7**), and -282290 (**8**), the names of the authors, and the literature citation.

Results and Discussion

A. Formation of Homoleptic Dipyridylamides of the Rare Earth Elements with the Focus of Different Metal Activation Routes. The reactions of lanthanide and group 3 metals with molten 2,2′-dipyridylamine can lead to three different types of homoleptic dipyridylamides of the rare earth elements. All three types have the formula $[Ln_2(Dpa)_6]$, with lanthanum alone being type I,[29] cerium to thulium representing type II, and ytterbium, lutetium, and scandium representing type III. All complexes **1**−**8** are formed according to the redox reaction

$$2Ln + 6(C_5H_4N)_2NH \xrightarrow{\text{melt}, \Delta T} [Ln_2(C_5H_4N)_2N)_6] + 3H_2 \quad (1)$$

Formation of the products can be achieved within a couple of hours to 1 or 2 days. For the growth of crystals suitable for X-ray analysis longer annealing times have to be chosen as given in the Experimental Section. Yields of the reactions are between 70 and 90% and were determined by thermogravimetry and on either washed samples (toluene, hexane) as well as after evaporation of excess DpaH.

---

(34) Sheldrick, G. M. *SHELXS-97, Program for the resolution of Crystal Structures*; University of Göttingen: Göttingen, Germany, 1997.

(35) Sheldrick, G. M. *SHELXL-97, Program for the refinement of Crystal Structures*; University of Göttingen: Göttingen, Germany, 1997.

Depending on the reactivity metal activation by Hg for amalgamation[31,36] is a long known and widely used suitable tool for dropping down the reaction temperatures and speeding up reactions[15−24] as are procedures including its formation like redox transmetalation metathesis.[37] The problem that the ligand as well as the products can start to decompose upon further heating can thereby be avoided. As amalgamation leads to incorporation of a hazardous volatile metal in the synthesis strategy, its replacement is attractive. It is a further impurity of the reaction mixtures and tends to give microcrystalline products with the necessity of long annealing times for suitable single crystals, reducing its value in these syntheses. The use of different and new activation methods has thus been studied with the oxidation with DpaH.

It is known that europium and ytterbium can be dissolved in liquid ammonia at normal pressure.[35,36] In addition to homoleptic hexammine complexes,[38] solvated electrons are formed that give dark blue solutions as for the alkaline metals.[39−41] Evaporation of the ammonia at temperatures above −33 °C allows one to regain the metals as very small particles and thus to get large pure surfaces. All passivation and impurities on the metal surfaces can thereby be avoided increasing the reactivity of the rare earth metals.[42,21] Reactions in liquid ammonia have also successfully been used in organometallic rare earth chemistry[43−45] including amide chemistry.[46−49] For 2,2′-dipyridylamine we have shown that no homoleptic dimeric complex but a molecular nitride [$Yb_3N(Dpa)_6$][$Yb(Dpa)_3$] is formed.[49] Hence it can only be used as a pure activation for the metals if conditions and products analogous to those for the solvent-free oxidations are intended. Furthermore, ammonia activation is limited by the solubility of the rare earth elements to europium and ytterbium if no high-pressure conditions can be provided.[36,50,51] For both europium and ytterbium, ammonia activation proved worthy for the syntheses of pyrazolates already[21] as well as for ytterbium dipyridylamide here.

As an additional activation type, rare earth metals can couple with microwaves. These strongly heat the metals providing reaction with the amine. Short pulses of microwaves have been introduced to activate the metal, probably by starting the reaction with the amine on the heated metal surface. Precaution has to be taken to work with short pulses only, as further heating of the metal leads to decomposition of the organic amine ligand. For DpaH a few pulses of 5 s (1200 W) proved suitable. Microwave activation is the fastest way but is hard to control, and decomposition of the organic amine can only barely be prevented, if the metal is heated too far, as the low yield of the holmium reactions illustrates.

All activation types result in a significant decrease of the reaction temperatures and allow the formation of rare earth dipyridylamides. Unactivated but otherwise identically arranged reactions did not work; viz., decomposition was observed at higher temperatures instead of product formation.

The melt conditions of the high temperature oxidation of the rare earth elements with an amine rely on the amine melt itself,[15−24] the latter being subsequently used up in stoichiometric reactions. This hinders complete reaction and complete crystallization of the products, whereas using a melt excess leads to phase impurities with the referring amine reactant. On the other hand, avoiding the melt as reactant by the use of a solvent can lead to co-coordination and thus heteroleptic complexes. Inert flux conditions already proved their value, e.g., in the formation of quinolinates.[52] For comparison we studied the influence of 1,2,3,4-tetrahydroquinoline as it neither dissolves the produts nor dissolves the metal reactants in reasonable amounts. Liquid 1,2,3,4-tetrahydroquinoline works with DpaH and all rare earth metals it was studied with. Though it is likely that a different substance needs to be found for amine ligands different from DpaH, it offers a suitable alternative to the other activation types here.

B. Crystal Structure Investigations on [$Ln_2(N(NC_5H_4)_2)_6$], Ln = Ce, Nd, Sm, Ho, Er, Tm, Yb, and Sc. Single-crystal X-ray investigations were used for all compounds to illustrate the differences between the two types of rare earth dipyridylamides presented in this work, as the powder patterns are almost identical. The compounds referred to as type II **(1−6)** all crystallize isotypically in the monoclinic crystal system with space group $P2_1/n$. To have comparable dimeric arrangements to type III, the nonstandard setting was kept. The compounds referred to as type III here (**7**, **8**) crystallize isotypically in the space group $P2_1/c$. The different ligand arrangement results both in a volume increase and in a density decrease at the border between type II and III (type II, Tm (**6**), $V = 2584.6(4) \times 10^6$ pm^3, $\rho = 1.746$ g /cm^3; type III, Yb (**7**), $2616.8(5) \times 10^6$ pm^3, $\rho = 1.735$ g/cm^3; see Table 1). In contrast, these parameters show a steady course according to the radii contraction of the lanthanide series within each type (**1−6** and **7**, **8**).

As described for [$Ln_2(Dpa)_6$], Ln = La, Gd, and Yb,[29] the rare earth ions in **1−8** are trivalent and coordinated in a distorted square antiprismatic manner by eight nitrogen atoms (Figure 1). The dimeric complexes are both homoleptic and exhibit complete nitrogen coordination. The Dpa ligands

---

(36) Gmelin, *Handbuch der anorganischen Chemie, Ergänzungsband der Seltenerdelemente*; Springer-Verlag: Berlin, 1978; Vol. 39, B6.
(37) Deacon, G. B.; Pain, G. N.; Tuong, T. D. *Polyhedron* **1985**, *4*, 1149−1150.
(38) Thompson, D. S.; Stone, M. J.; Waugh, J. S. *J. Phys. Chem.* **1966**, *70*, 934−935.
(39) Weyl, W. *Poggendorff Ann.* **1864**, *121*, 601.
(40) Kraus, C. A. *J. Am. Chem. Soc.* **1908**, *30*, 1323−1325.
(41) Symons, M. C. R. *Chem. Soc. Rev.* **1976**, *5*, 337−355.
(42) Hadenfeldt, C.; Jacobs, H.; Juza, R. *Z. Anorg. Allg. Chem.* **1970**, *379*, 144−156.
(43) Fischer, E. O.; Fischer, H. *Angew. Chem.* **1964**, *76*, 134; *Angew. Chem., Int. Ed. Engl.* **1964**, *3*, 132.
(44) Hayes, R. G.; Thomas, J. L. *J. Am. Chem. Soc.* **1969**, *91*, 6876−6877.
(45) Evans, W. J.; Greci, M. A.; Ziller, J. W. *J. Chem. Soc., Dalton Trans.* **1997**, 3035−3039.
(46) Cetinkaya, B.; Hitchcock, P. B.; Lappert, M. F.; Smith, R. G. *J. Chem Soc., Chem. Commun.* **1992**, 932−934.
(47) Müller-Buschbaum, K. *Z. Anorg. Allg. Chem.* **2004**, *630*, 895−899.
(48) Quitmann, C. C.; Müller-Buschbaum, K. *Z. Anorg. Allg. Chem.* **2004**, *630*, 2422−2430.
(49) Quitmann, C. C.; Müller-Buschbaum, K. *Angew. Chem.* **2004**, *116*, 6120−6122; *Angew. Chem. Int. Ed.* **2004,** *43*, 5994−5996.
(50) Jacobs, H.; Fink, U. *Z. Anorg. Allg. Chem.* **1978**, *438*, 151−159.
(51) Hadenfeldt, C.; Gieger, B.; Jacobs, H. *Z. Anorg. Allg. Chem.* **1974,** *403*, 319−326.
(52) Deacon, G. B.; Junk, P. C.; Leary, S. *Z. Anorg. Allg. Chem.* **2005**, *631*, 2647−2650.

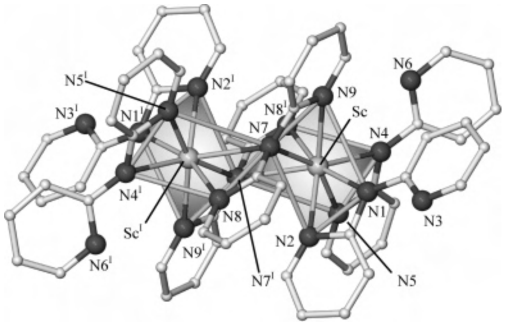

Figure 1. Distorted square antiprismatic coordination spheres of nitrogen atoms around scandium atoms as well as the aromatic ring systems in $[Sc_2(Dpa)_6]$ (**8**). Lines between the nitrogen atoms do not represent bonds but show the distorted antiprism. The Sc atoms are depicted as gray balls, the N atoms as small dark balls, and C atoms as small light gray balls; H atoms are left out for clarity. Symmetry operation: (I) $-x$, $1 - y$, $-z$.

Chart 2. Depiction of the Dimeric Arrangement in $[Ln_2(N(C_5H_4N)_2)_6]$ with a Symmetric Bridging of the 1,3/1,3-Double Chelating Dipyridylamide Ligands

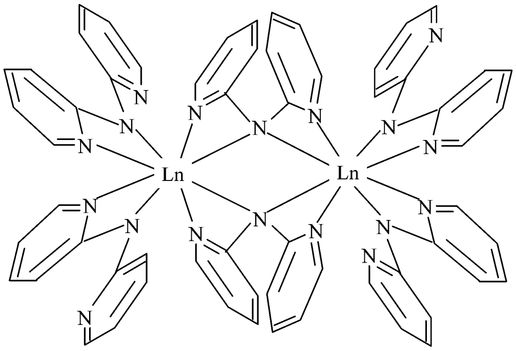

Table 2. Selected Distances/pm and Angles/deg between Atoms of $[Ln_2(Dpa)_6]$, Ln = Ce (**1**), Nd (**2**), Sm (**3**), Ho (**4**), Er (**5**), Tm (**6**), Yb (**7**), and Sc (**8**) and $Dpa^- = (C_5H_4N)_2N^-$ (Deviations in Parentheses)

atoms	**1**	**2**	**3**	**4**
Ln−N1	246.8(5)	244.0(4)	242.8(4)	236.6(5)
Ln−N2	264.1(5)	259.2(4)	254.0(4)	246.4(5)
Ln−N4	251.2(4)	247.2(4)	243.2(4)	238.4(5)
Ln−N5	259.8(4)	256.1(4)	252.9(4)	245.2(5)
Ln−N7	241.1(4)	261.6(4)	258.7(4)	254.6(5)
Ln−N8[a]	261.6(5)	256.7(4)	255.3(4)	244.9(5)
Ln−N9	261.4(4)	258.2(4)	252.8(4)	248.7(5)
Ln−N7[a]	272.9(4)	268.1(4)	262.8(4)	251.6(5)
Ln−Ln[a]	416.9(1)	410.3(1)	404.8(1)	395.1(1)
N1−Ln−N4	87.3(2)	87.2(2)	86.9(1)	86.1(2)
N1−Ln−N9	79.2(2)	79.5(2)	78.6(1)	78.8(2)
N2−Ln−N7	92.3(2)	85.5(2)	91.1(1)	87.3(2)
N2−Ln−N5	71.6(2)	72.2(2)	72.5(1)	73.4(2)
N9−N7−C21[b]	143.1(5)	141.7(3)	145.3(4)	139.1(3)

atoms	**5**	**6**	**7**	**8**
Ln−N1	236.7(9)	235.5(4)	234.0(5)	223.3(2)
Ln−N2	248(1)	244.4(4)	241.6(5)	233.0(2)
Ln−N4	242(1)	238.3(3)	240.7(5)	237.0(2)
Ln−N5	243(2)	243.1(4)	236.8(5)	225.5(2)
Ln−N7	250(1)	251.2(4)	246.2(5)	231.8(2)
Ln−N8[a]	243(1)	242.1(4)	237.2(5)	226.9(2)
Ln−N9	247(1)	247.0(4)	244.1(5)	234.2(2)
Ln−N7[a]	251.3(9)	251.7(4)	256.9(5)	262.1(2)
Ln−Ln[a]	393.4(1)	392.6(1)	391.6(1)	389.3(1)
N1−Ln−N4	86.1(4)	86.2(1)	87.9(2)	87.31(6)
N1−Ln−N9	79.0(4)	87.2(1)	87.1(2)	87.09(6)
N2−Ln−N7	88.8(4)	86.7(1)	89.5(2)	83.17(5)
N2−Ln−N5	73.4(4)	73.3(1)	78.2(2)	77.34(6)
N9−N7−C21[b]	139(1)	139.8(3)	143.7(4)	144.79(9)

[a] Symmetry operation: $-x$, $1 - y$, $-z$. [b] Torsion angle, reflecting distortion of the double chelating Dpa ligands.

coordinate in two different ways. End-on amide ligands exhibit a single 1,3-chelating coordination to one metal center, with one pyridylring being noncoordinating. This coordination mode is similar to aminopyridinato complexes[30] that do not contain the second pyridyl ring (see Chart 1). Linking amide ligands in **1**−**8** show a double 1,3/1,3-chelating mode with the central N atom μ_2-connecting two metal ions and distorting the Dpa ligand (see Chart 2). The lanthanum compound contains four double chelating ligands resulting in a CN (coordination number) of 10 for La.[29] All other lanthanide and group 3 dipyridylamides presented here contain only two double chelating Dpa ligands. Thus they exhibit a CN of 8 or even less. A tendency toward a reduced CN of 7 + 1 can be seen for Sc already, as an asymmetric bridging of the linking ligands is observed. The smaller the rare earth ion, the stronger this asymmetry becomes (Sc−N (**8**) = 231.8(2) and 262.1(2) pm, Ce (**1**) = 265.7(4) and 272.9(4) pm). The Ln−N distances in **1**−**8** reflect the complete course of ionic radii [53] of the lanthanide series. The 1,3-single chelating ligands exhibit the shortest Ln−N distances, and the linking double chelating ligands, longer Ln−N distances (see Table 2). The two structure types present one major difference; viz., type II (**1**−**6**) shows longer distances to the pyridyl N atoms whereas type III (**7**, **8**) exhibits shorter distances to the pyridyl ring N atom compared to the N atom μ_2-linking both pyridyl rings. The overall Ln−N distances match well with other eight-coordinate Ln−N complexes such as phthalocyanines[5−7] or pyridylbenzimidazolates[17−19] and the known dipyridylamides of lanthanum (La−N distances of 254−290 pm) and gadolinium (Gd−N distances of 242−259 pm).[29]

The square-antiprismatic coordination is distorted. This distortion increases with the ionic radius of the lanthanide ion from **8** to **1**, which is illustrated by the interatomic N−Ln−N angles. The referring angles for Ce (**1**) range from 77.0(1) to 95.3(1)°, for Nd (**2**) from 75.5(1) to 91.6(1)°, and those from Tm (**6**) on these angles are nearly identical with 84.6(1)−87.2(1)° to Sc (**8**) with 83.17(6)−86.73(6)°. Thus, distortion of the polyhedra and symmetry of the Ln−N−Ln bridging are contrary.

The most prominent difference apart from coordination is the metal metal distance in the dimers. Lanthanum with a CN of 10 (type I) exhibits the shortest Ln−Ln distance of all dipyridylamides with 367 pm though it is the largest Ln cation.[29] For the CN of 8 the opposite trend concerning the rare earth radius is observed. As expected Sc (**8**) shows the shortest Ln−Ln distance with 389.3(1) pm, whereas the Ce (**1**) exhibits the largest Ln−Ln distance of 416.9(1) pm (Figure 2).

Figures 3 and 4 exhibit depictions of the different crystal structure types II (**1**−**6**) and III (**7**, **8**). They show that a transformation of one type into the other is not possible. The crystal structure of the Yb complex (**7**) needed to be revised as the rotational positions of the noncoordinating pyridyl rings can now be defined.

---

(53) Shannon, R. D. *Acta Crystallogr.* **1976**, *A32*, 751−767.

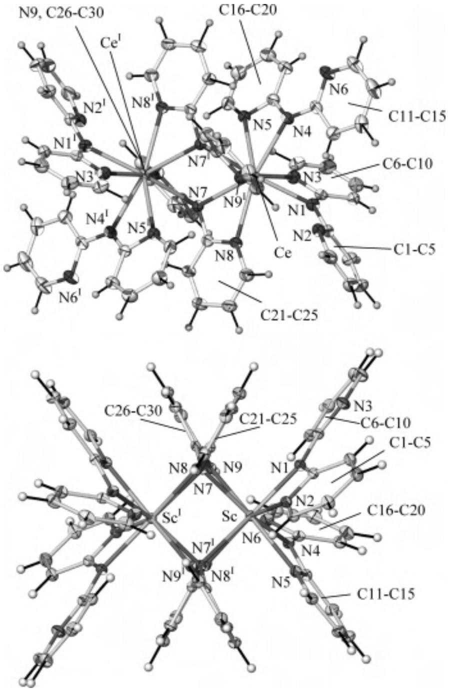

Figure 2. Dimeric molecular units of [$Ce_2(Dpa)_6$] (**1**, top) and [$Sc_2(Dpa)_6$] (**8**, bottom). The thermal ellipsoids reflect 50% of the probability level of the atoms. Symmetry operation: (I) $-x$, $1 - y$, $-z$.

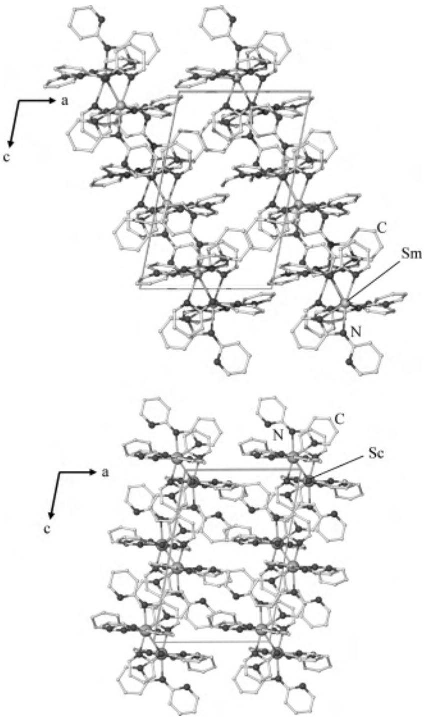

Figure 3. Crystal structures of the types II and III dipyridylamides [Sm_2-$(Dpa)_6$] (**3**, top) and [$Sc_2(Dpa)_6$] (**8**, bottom) with a view along $[0\bar{1}0]$. The Ln atoms are depicted as large gray balls, the N atoms as dark balls, and the C atoms as small light balls. H atoms are left out for clarity. **3** is depicted in the setting $P2_1/n$, and **8** in the setting $P2_1/c$ reflecting the different orientations of the dimeric units in both types.

C. Spectroscopic Investigations on [$Ln_2(N(NC_5H_4)_2)_6$], Ln = Ce, Nd, Sm, Ho, Er, Tm, Yb, and Sc. The dipyridylamides [$Ln_2(Dpa)_6$] (**1**−**8**) were investigated spectroscopically with mid-IR, far-IR (and Raman for **1**, **3**, **4**, and **6**) techniques. Compounds **2**, **5**, **7**, and **8** gave no Raman spectra. Both far-IR and Raman spectra show a series of bands that cannot be identified with the neutral ligand[29] and represent the Ln−N stretching modes. E.g., for the group 3 metal Sc (**8**) the far-IR bands are 264, 244, 234, 216, and 185 cm^{-1} and thereby shifted in comparison to the respective bands of the lanthanides. All are in the region of known Ln−N vibrations.[6,24,17−21,54] Due to the distortion of the square antiprismatic coordination spheres, the Raman spectra are nearly plain in the referring region and show only one vibration band that is interpreted as an Ln−N vibration. The expected hypsochromic shift corresponding to the expectations of the radii effect of the rare earth elements[53] and can only be found for one of these bands (far-IR, cm^{-1}: Ce (**1**), 235; Nd (**2**), 244; Sm (**3**), 249; Ho (**4**), 254; Er (**5**), 255; Tm (**6**), 257). Other far-IR bands as well as the Raman band remain nearly unchanged from **1**−**8** though they clearly do not derive from the amine itself, as it does not show bands in the referring region.[29] Distinct differences in the far-IR spectra between the two types of dipyridylamides II and III cannot be observed.

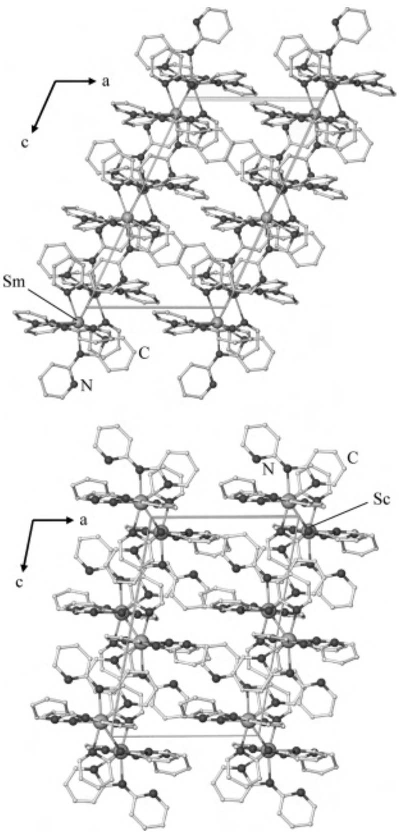

Figure 4. Crystal structures of the types II and III dipyridylamides [Sm_2-$(Dpa)_6$] (**3**, top) and [$Sc_2(Dpa)_6$] (**8**, bottom) with a view along $[0\bar{1}0]$ both in the standard setting $P2_1/c$. The Ln atoms are depicted as large gray balls, the N atoms as dark balls, and the C atoms as small light balls. H atoms are left out for clarity. Both the resulting large β angle for **3** and the different orientations of the dimeric units are shown.

Concerning the ligand vibrations,[54] a further comparison of the spectra with the bands of the free ligand shows a hypsochromic shift of several IR bands of about 10 wave-

---

(54) Weidlein, J.; Müller, U.; Dehnicke, K. *Vibrational frequencies, transition metal elements*; Georg Thieme Verlag: Stuttgart, Germany, 1986.

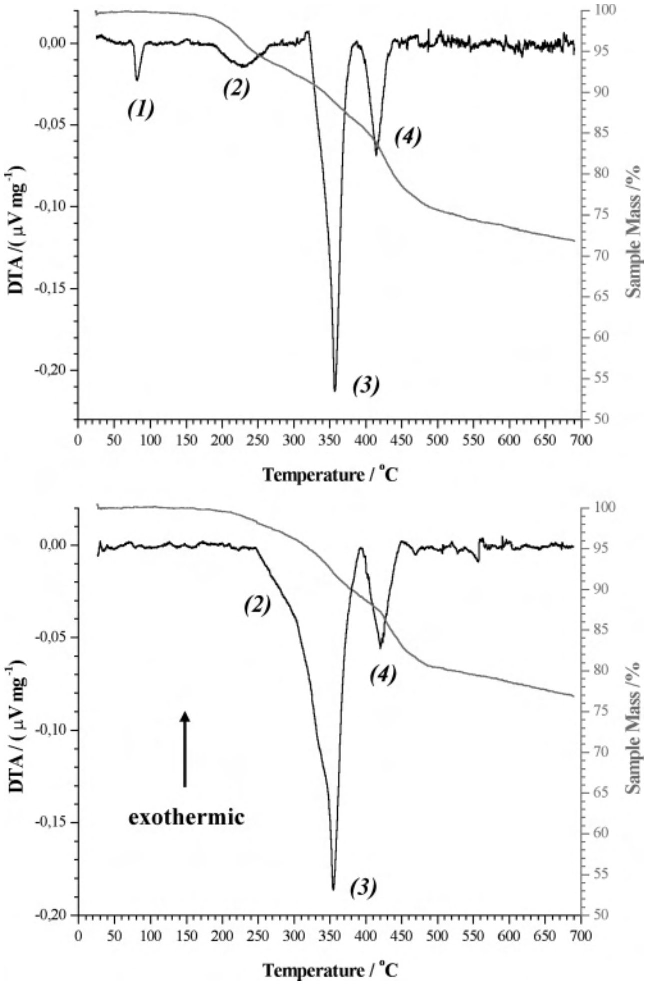

Figure 5. Thermal decompositions of 21.2 mg of bulk [$Tm_2(Dpa)_6$] (**6**, top) and 18.5 mg of sublimed [$Tm_2(Dpa)_6$] (**6**, bottom) investigated by simultaneous DTA/TG in the temperature range 20−700 °C with a heating rate of 10 °C/min in a continuous Ar flow of 60 mL/min. Heat flow signals deriving from excess DpaH are weaker or missing for the purified sample.

numbers as well as a certain splitting of IR bands. The IR band at 1600 cm^{-1} is characteristic for C═C vibrations and shifted by 10 wavenumbers compared to dipyridylamine (1594 cm^{-1}) due to weakening of the aromatic ring system. The observation of intense bands in the region of 1500−1200 cm^{-1} is expected and comparable to other heterocycles.[55]

D. Thermal Investigations on [$Ln_2(N(NC_5H_4)_2)_6$], Ln = Ho, Er, Tm, Yb, and La (9). Simultaneous DTA and TG [56] measurements as well as DTA/TG combined with mass spectrometry were carried out to investigate the thermal behavior of the Ln dipyridylamides. In addition to the bulk products of the melt syntheses of **4**−**7** and **9**, the crystalline products of **4** and **6** were further purified from additional dipyridylamine by evaporating the amine and also investigated with simultaneous DTA/TG. Yield determination by thermal gravimetry on the bulk products compared to weight determinations gives consistent results.

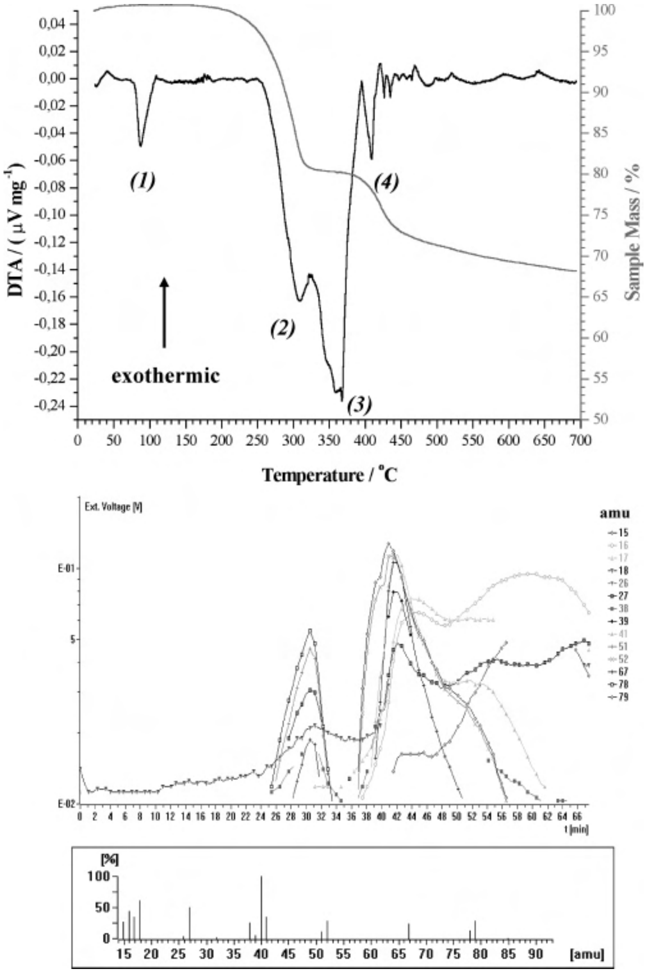

Figure 6. Thermal decompositions of 49.3 mg of bulk [$Er_2(Dpa)_6$] (**5**) investigated by simultaneous DTA/TG (top) and mass spectrometry (middle and bottom) in the temperature range 20−700 °C with a heating rate of 10 °C/min in a continuous Ar flow of 60 mL/min up to $m/z = 95$. All four heat flow signals can be detected. A direct correlation of the detected masses in the mass spectrogram (middle) and the DTA/TG can be drawn, as both depictions are in scale. The 100% mass (bottom, $m/z = 40$) can be identified with the flow gas argon.

The investigation of the bulk as well as of purified products shows that the samples contain different amounts of excess DpaH. Bulk **4**−**7** and **9** display an endothermic peak with no correlated mass loss as the first signal 1 that can be identified as the melting point of DpaH (see Figures 5 and 6). As the DpaH content of the purified products **4** and **6** is very low, the melting point of DpaH cannot be observed in the referring heat flows. An endothermic signal 2 is following signal 1 between 225 and 235 °C in all measurements. It can be identified with the boiling point of DpaH (expected: 238 °C) and correlates to different amounts of excess dipyridylamine leaving the sample (see Table 3 for detailed information). Beyond the boiling point of excess DpaH and below their own melting points, some Ln−dipyridylamides already become partly volatile, which can bee seen in a low but steady mass loss in the TG. This is most prominent for Tm in **6** (6% for the bulk product and 8% for the purified sample), whereas it is almost not present for Er in **5**, Yb in **7**, and La in **9**. All rare earth dipyridylamides melt congruently, again identified by a sharp endothermic peak with no referring mass loss (signal 3). The significant difference in

---

(55) Schrader, B. *Raman/Infrared Atlas of Organic Compounds*, 2nd ed.; Wiley VCH: New York, 1989.

(56) Hemminger, W. F.; Cammenga, H. K. Methods of thermal analysis; Springer-Verlag: Berlin, 1989.

Table 3. Results of the Simultaneous DTA/TG Investigations of $[Ln_2(Dpa)_6]$, Ln = Ho (**4**, Bulk and Purified), Er (**5**), Tm (**6**, Bulk and Purified), Yb (**7**), and La (**9**) and $Dpa^- = (C_5H_4N)_2N^-$

param	Ho (**4**) bulk	Ho (**4**) purified	Er (**5**) bulk	Tm (**6**) bulk	Tm (**6**) purified	Yb (**7**) bulk	La (**9**) bulk
heat flow signal 1/°C	85 (mp DpaH)		80 (mp DpaH)	80 (mp DpaH)		85 (mp DpaH)	85 (mp DpaH)
mass loss/%							
heat flow signal 2/°C	235 (bp DpaH)	235 (bp DpaH)	240 (bp DpaH)	225 (bp DpaH)	230 (bp DpaH)	235 (bp DpaH)	230 (bp DpaH)
mass loss/%	22	6	19	6	3	29	16
heat flow signal 3/°C	335 (mp 4)	335 (mp 4)	320 (mp 5)	320 (mp 6)	315 (mp 6)	325 (mp 7)	280 (mp 9)
mass loss/%							
heat flow signal 4/°C	410 (dec 4)	410 (dec 4)	385 (dec 5)	395 (dec 6)	390 (dec 6)	370 (dec 7)	340 (dec 9)
mass loss/%	10	22	12	21	24	11	14

the melting points of the lanthanum compound and the other dipyridylamides can possibly be explained by the different structure type of $[La_2(Dpa)_6]$ including a different coordination number.[29] Upon further heating, the rare earth dipyridylamides decompose, the mass loss depending on the rare earth ion and the amount of excess DpaH in the sample (signal 4). An extrapolation of these mass losses on 100% pure samples indicates that the bulk products with high amounts of excess DpaH also contain excess metal in all measurements. Both the melting points and decomposition temperatures are high concerning organic amine ligands but correspond to other homoleptic rare earth amides and amides with a pure nitrogen surrounding investigated by thermal analysis.[18,23,24,57]

Further confirmation is provided by the simultaneous investigation with mass spectrometry. This was carried out for the bulk sample of Er (**5**). The MS investigation supports the identification of all DTA signals 1−4. Figure 6 correlates the results of simultaneous DTA/TG and mass spectrometry. For the melting point of dipyridylamine, no mass signal can be detected. Corresponding to the boiling point of excess DpaH, the mass signal for $DpaH^+$ ($m/z = 171$) is detected after 25 min (25 min = 270 °C; signal 2 in the heat flow) in addition to several fragmentation products (pyridyl ring $C_5H_4N^+$ $m/z = 78$; ring fragments $C_4H_4N^+$ $m/z = 67$, $C_4H_3^+$ $m/z = 51$, $C_3H_2^+$ $m/z = 38$, $C_2H_3^+/HCN^+$ $m/z = 27$). Between the heat flow signals 2 and 4 the mass spectrogram exhibits no mass signals. Upon decomposition of the product complex **5** (37 min = 390 °C; signal 4) a set of mass signals correlating to the decomposition of the coordinating amide ligands is detected excluding the mass of the DpaH molecule (pyridyl ring $C_5H_5N^+$ $m/z = 79$; ring fragments $C_4H_4^+$ $m/z = 52$, $C_2H_3N^+/NCHN^+$ $m/z = 41$, $C_3H_3^+$ $m/z = 39$, $C_2H_3^+/HCN^+$ $m/z = 27$). As observed for the decomposition of other N-heterocycles,[18,23,24,57] ammonia-related masses (NH_3^+, NH_2^+, NH^+, $m/z = 17, 16, 15$) are detected, their amount increasing upon further heating. This supports the assumption that the dipyridylamide complexes have a thermal stability up to the border at which the C−N bonds start to break and the ligand decomposes in whole, even releasing ammonia fragments.

Conclusions

In reactions of rare earth metals with organic amines, the large differences in the melting points of the metals compared to the organic ligands prove a barrier for this solid-state chemistry reaction route in melts. Therefore, different activation types for the metals were investigated for the formation of rare earth dipyridylamides: amalgam formation and electride and microwave activation. While amalgam formation is most widely used including rare earth metals, its toxicity makes a replacement attractive. Electride formation implies solubility of the Ln elements in liquid ammonia and, avoiding higher pressures, is limited to europium and ytterbium only. Excess ammonia can be evaporated otherwise coordination of ammonia can easily occur upon reaction in ammonia. Coupling of the metals to microwaves is also possible and results in immediate strong reactions. The intense heating of the metal is hard to control and can result in decomposition of the organic ligand and products. All activation types result in a distinct decrease of the reaction temperatures needed for the subsequent melt reactions compared to unactivated rare earth metals. Formation of the dimeric Dpa complexes is also possible in 1,2,3,4-tetrahydroquinoline, which proves a reasonable alternative.

Preparation of the lanthanide series revealed a third, previously undiscovered structure type of dipyridylamides. The borders between the three types of homoleptic rare earth dipyridylamides are drawn by the ionic radii and are located between lanthanum and cerium and between thulium and ytterbium, respectively. Only the lanthanum compound exhibits a nitrogen CN of 10, whereas the other two types throughout the lanthanide series show a CN of 8 each, with Sc as the smallest ion tending to 7 + 1.

Concerning the organic ligand, rare earth dipyridylamides have relatively high melting points and even higher thermal stabilities up to decomposition of C−C and C−N bonds.

Acknowledgment. We thank Prof. Gerd Meyer (Inst. für Anorg. Chemie, Universität zu Köln) for his generous support, Prof. Ladislav Bohaty (Inst. für Kristallographie, Universität zu Köln) for his help to verify the nonisotypic character of the sturcture types, the Deutsche Forschungsgemeinschaft for funding this work through the Schwerpunktprogramm 1166 “Lanthanoid-spezifische Funktionalitäten in Molekül und Material”, and the Fonds der Chemischen Industrie for a Ph.D. fellowship.

Supporting Information Available: Tables of atomic coordinates, thermal parameters, atom distances, interatomic angles, and detailed crystallographic data for **1**−**8** and additional depictions of the crystal structures and thermal decompositions. This material is available free of charge via the Internet at http://pubs.acs.org.

IC0514795

---

(57) Quitmann, C. C.; Müller-Buschbaum, K. *Z. Kristallogr.* **2005**, *220*, 158−165.